Supporting Information

Zwitterionic Phenyl Layers: Finally, Stable, Anti-Biofouling Coatings that Do Not Passivate Electrodes

*Alicia L. Gui,† Erwann Luais,‡ Joshua R. Peterson, J. Justin Gooding**

School of Chemistry and Australian Centre for NanoMedicine, The University of New South Wales, Sydney, NSW 2052, AUSTRALIA

* E-mail: justin.gooding@unsw.edu.au

Present Addresses

†Current address: Institut für Reine und Angewandte, Carl von Ossietzky Universität Oldenburg, Oldenburg, 26111, Germany.

‡Current address: GREMAN, Université François Rabelais, Tours, 37200, France.

Electrochemistry of Reductive Adsorption of In Situ Generated Phenyl Phosphorylcholine (PPC) Diazonium Salt and Phenyl 4-(2-(2-(2-Hydroxy -ethoxy)-ethoxy)ethyl) (OEG-Ph) Diazonium Salt on Glassy Carbon

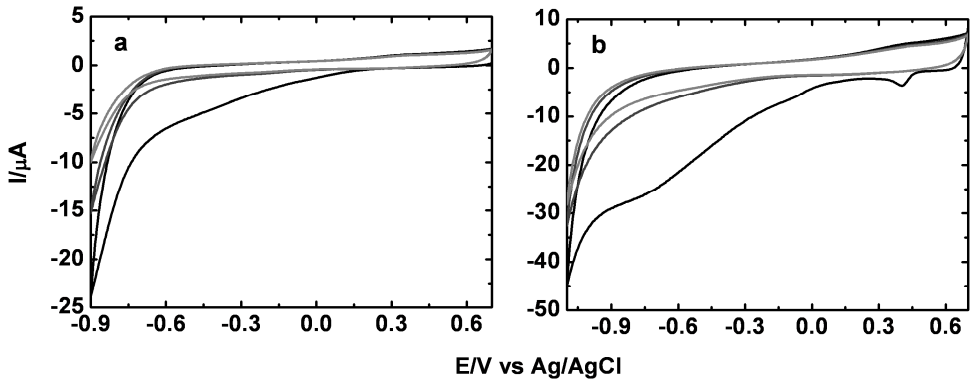

Figure SI 1. Cyclic voltammetry of reductive adsorption of *in situ* generated phenyl phosphorylcholine (PPC) diazonium salt (a), and phenyl 4-(2-(2-(2-hydroxy-ethoxy)-ethoxy)ethyl) (OEG-Ph) diazonium salt (b) salt on glassy carbon electrode, the 1st scan (black), 2nd scan (dark gray) and 3th scans (gray). Experimental conditions: 5 mM corresponding aniline derivative, 0.1 M HBF_4 and 1 equiv (5 mM) of $NaNO_2$ in aqueous solution, scan rate = 100 mV/s.

As the Figure SI 1 shows, the initial cathodic scan of glassy carbon electrode in the solution containing *in situ* generated PPC diazonium salt begins to exhibit a negative current increase at about +0.15 V. The cathodic current continues to increase until a much sharper intensity growth appearing at around -0.75 V, which is attributed to the hydrogen evolution. Although there is no distinct reduction peak observed, the dramatic decrease of cathodic current between +0.15 to -0.75 V in the second scan has indicated the passivation of electrode surface by the grafted phenyl layers. The reductive adsorption CV of *in situ* generated OEG-Ph diazonium salt is presented in Figure SI 1b. A small reduction peak at around +0.45 V followed by a large broad wave extending from -0.3 V to -0.9 V can be identified in the first scan. The observation of multiple reduction peaks of other *in situ* generated aryl diazonium salts on carbon surface is also reported in literature,[1] but the origin of this phenomenon has not been explained. However, the two peaks completely disappeared in the second cycle. This suggests the presence of grafted OEG-Ph layers, which restrain further electrochemical reduction of aryl diazonium salts.

XPS Characterization of Bare Glassy Carbon Surface

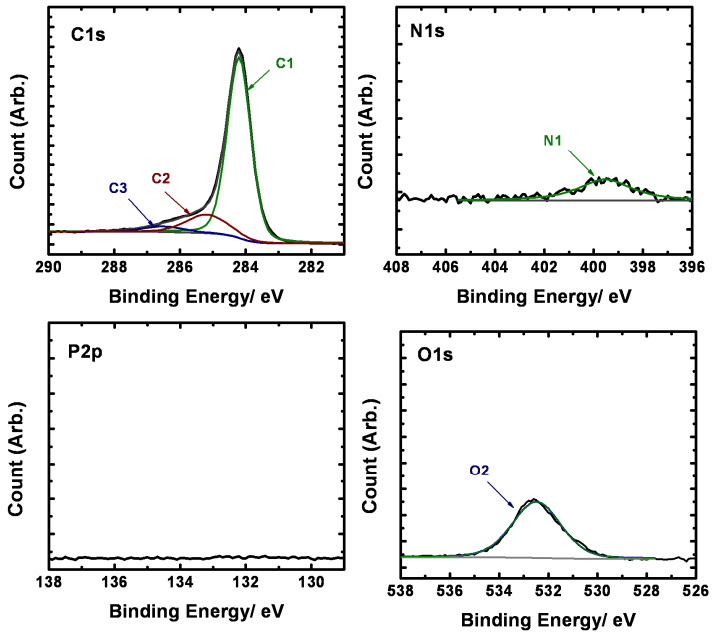

Figure SI 2 X-ray photoelectron spectrum of bare glassy carbon surface. The C1s, N1s, O1s and P2p narrow scans.

Table SI 1. XPS Atomic percentage comparison of C,N,O and P between bare glassy carbon surface and PPC-GC surface

Core-level	C1s			N1s		O1s		P2p
Peaks	*C1*	*C2*	*C3*	*N1*	*N2*	*O1*	*O2*	*P*
At % on Bare GC	64.40 (*s*=0.15)	13.42 (*s*=0.17)	5.36 (*s*=0.13)	1.32 (*s*=0.25)	-	-	15.50 (s=0.09)	0.00
At % on PPC-GC	24.24(*s*=0.08)	16.58 (*s*=0.34)	19.19(*s*=0.29)	0.63 (*s*=0.18)	3.18 (*s*=0.06)	14.14 (*s*=0.15)	18.69 (*s*=0.54)	3.34 (*s*=0.04)

XPS Characterization of Phenyl 4-(2-(2-(2-hydroxy-ethoxy)-ethoxy)- ethyl) Grafted Glassy Carbon (OEG-Ph-GC)

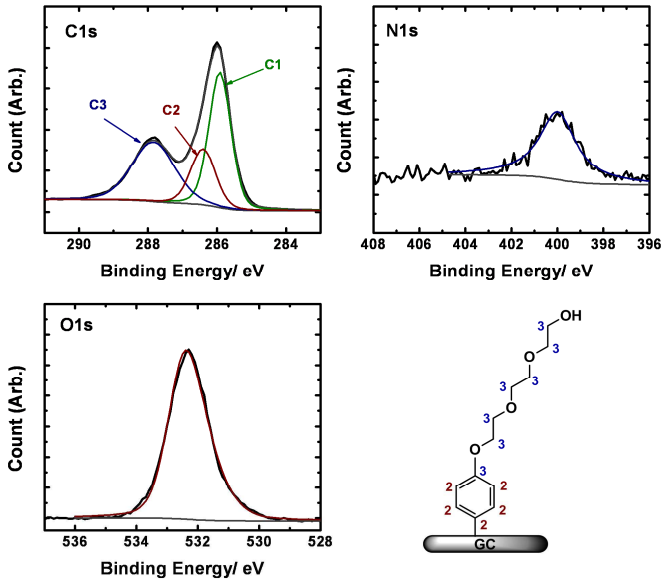

Figure SI 3. X-ray photoelectron spectrum of phenyl 4-(2-(2-(2-hydroxy-ethoxy)-ethoxy)ethyl) (OEG-Ph) layers on glassy carbon surface. The C1s, N1s, O1s narrow scans.

Figure SI 3 above contains the C1s, N1s and O1s narrow scans from XPS measurement of OEG-Ph-GC. Three peaks fitted under the C1s spectrum are respectively centered at 285.1 eV (C1), 285.6 (C2) and 287.0eV (C3). The peak C3 arises from the six aliphatic carbon atoms of the tri(ethylene glycol) chain and the one aromatic carbon atom which it bonds to. The peak C2 is from the remaining five aromatic carbon atoms. The C1 peak is from the glassy carbon substrate. There is only one peak in the N1s narrow scan observed at about 400.2 eV. As mention previously, this peak attributed to an azo signal from the multilayers structure.[2, 3] The O1s narrow is observed with one peak at 532.5 eV. The oxygen signal was shifted compared to oxygen signal on bare glassy carbon surface at 531.9 eV. The atomic ratio of oxygen and carbon calculated from XPS measurement is much higher than the theoretical value derive from OEG-Ph molecular structure. This suggests the peak at 532.5 contains signal from surface oxide.

Electrochemical Stability of PPC-GC and OEG-Ph-GC Surfaces

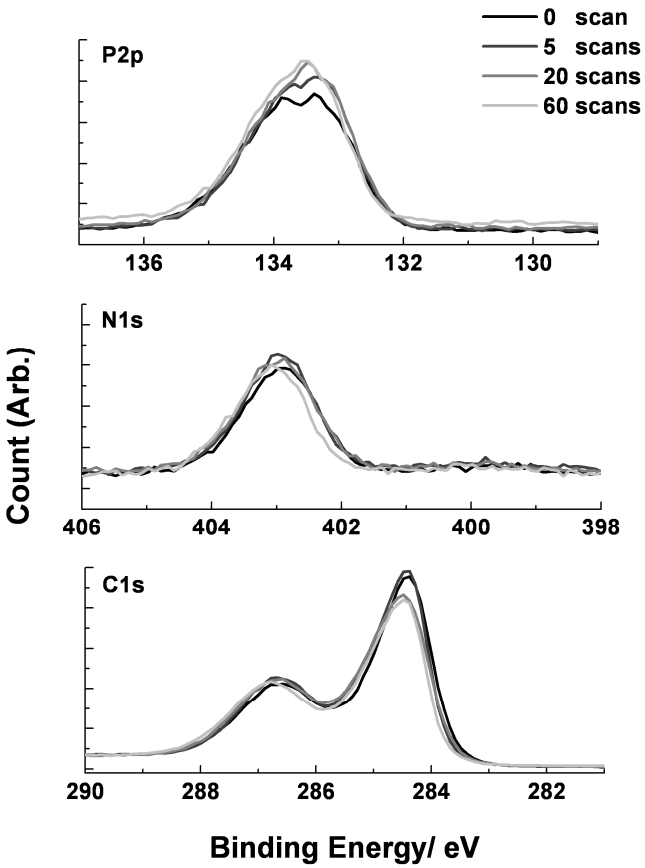

Figure SI 4. X-ray photoelectron spectrum of surface PPC-GC. The comparison of the changes of P2p, N1s and C1s narrow scans after surface been treated with different number of multiple CV scans in 0.1 M KCl aqueous solution between – 1.0 V to 0.8 V at scan rate of 100 mV/s.

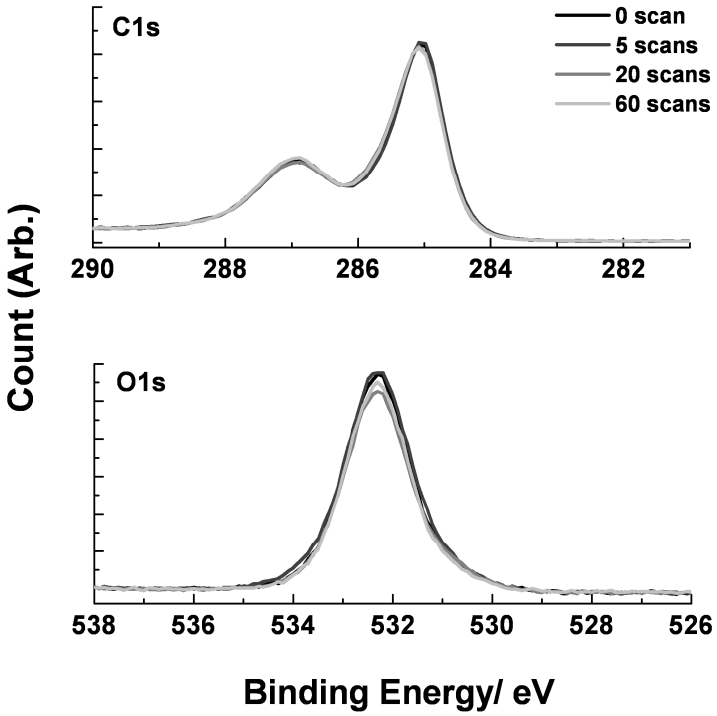

Figure SI 5. X-ray photoelectron spectrum of surface OEG-Ph-GC. The comparison of the changes of C1s, and O1s narrow scans after surface been treated with different number of multiple CV scans in 0.1 M KCl aqueous solution between – 1.0 V to 0.8 V at scan rate of 100 mV/s.

PPC-GC and OEG-Ph-GC surfaces were subjected to electrochemical stability testing. The surfaces were treated with continuous cyclic voltammetry scans in a potential range of -1 V to 0.8 V for various numbers of cycles in 0.1 M KCl aqueous solution. The changes in surface chemical composition of the PPC-GC and OEG-Ph-GC after cyclic voltammetry scans ware monitored by XPS. As shown in Figure SI 4 and 5, after been treated with up to 60 cycles of scans, the spectrum exhibit only minor signal changes in terms of intensities and the binding energy of the peaks for both PPC-GC and OEG-Ph-GC. These results suggest the molecular structure of the surface grafted PPC and OEG-Ph withstand the electrochemical treatment above, which is a good indication of the stability of PPC and OEG on the GC surface.

Cyclic Voltammetry Comparison of PPC-GC, Mix-GC, OEG-Ph-GC, OEG-SAM-Au and C12-SAM-Au Surfaces in Aqueous Solution Containing Soluble Redox Probes

The cyclic voltammetry (CV) responses of PPC-GC, Mix-GC, OEG-Ph-GC, OEG-SAM-Au and C12-SAM-Au surfaces to the two soluble redox probes were also investigated. CV is useful in probing the integrity of the functionalized layers on the electrode surfaces.

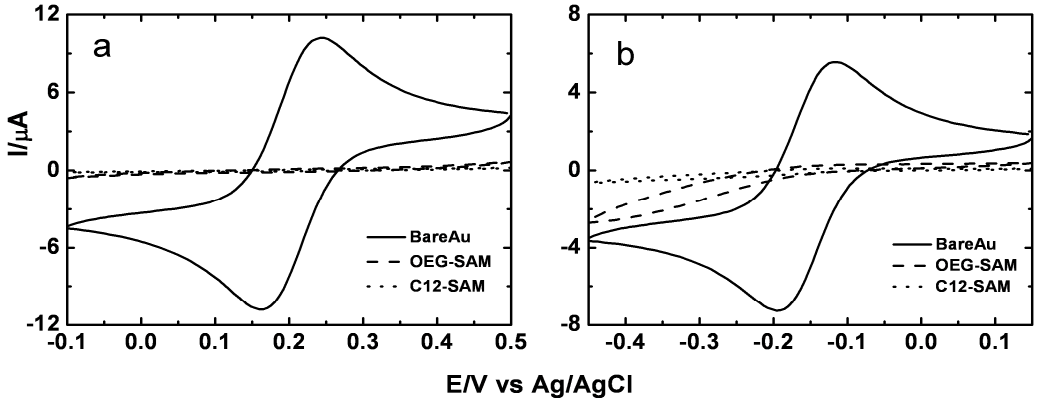

Figure SI 6. Cyclic voltammetry of gold electrodes in (a) 1 mM $Fe(CN)_6^{3-}$ with 0.1 M KCl aqueous solution (b) 1 mM $Ru(NH_3)_6^{3+}$ with 0.1 M KCl aqueous solution. Comparison of bare surface (solid curve) and surface modified with OEG-SAM (dash curve) and C12-SAM (dot curve)

As shown by Figure SI 6a, the electrochemistry of $Fe(CN)_6^{3-}$ is completely suppressed at both OEG-SAM-Au and C12-SAM-Au. In Figure SI 6b, the current of the redox reaction $Ru(NH_3)_6^{3+}$ is also completely attenuated on surface C12-SAM-Au. However, the OEG-SAM-Au is shown to be slightly more accessible than C12-SAM-Au to $Ru(NH_3)_6^{3+}$. The electrochemical behaviors of $Fe(CN)_6^{3-}$ and $Ru(NH_3)_6^{3+}$ on OEG-SAM-Au and C12-SAM-Au surfaces shown above are consistent to what is expected to be on the ordered and closely packed alkanethiol SAMs[4].

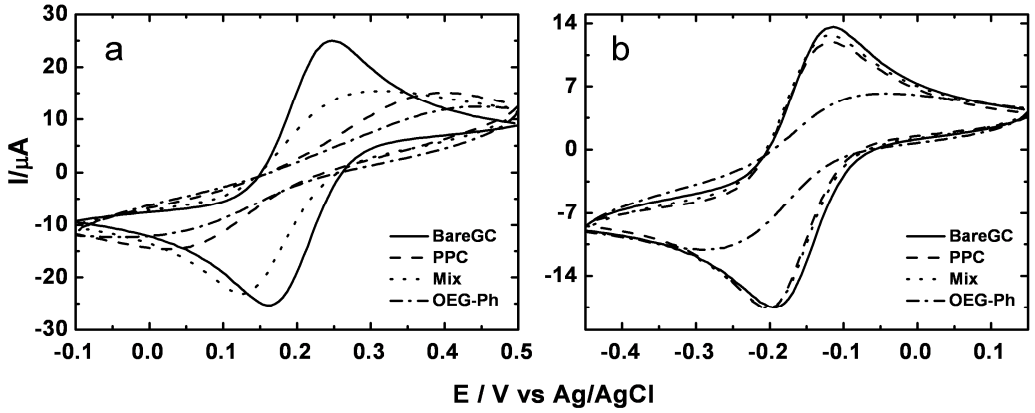

Figure SI 7. Cyclic voltammetry of glassy carbon electrodes in (a) 1 mM $Fe(CN)_6^{3-}$ with 0.1 M KCl aqueous solution (b) 1 mM $Ru(NH_3)_6^{3+}$ with 0.1 M KCl aqueous solution. Comparison of bare surface (solid curve) and surface modified with PPC layers (dash curve); Mix layers (dot curve); OEG-Ph layers (dash dot curve).

Figure SI 7 a and b show the electrochemical behavior of $Fe(CN)_6^{3-}$ and $Ru(NH_3)_6^{3+}$ on PPC-GC, Mix-GC and OEG-Ph-GC surfaces. In comparison to OEG-SAM-Au and C12-SAM-Au, the attenuation of $Fe(CN)_6^{3-}$ and $Ru(NH_3)_6^{3+}$ current is generally much less than on these aryl diazonium salts derived layers. For PPC-GC and Mix-GC, this phenomenon should mostly be related to the fact that the PPC and Mix layers are much thinner than SAMs and thus provide a limited electron tunneling barrier. Another factor could be that the packing of phenyl derivative layers are much less compact than SAMs, which is particularly likely to be the case for OEG-Ph-GC, and also PP-GC and Mix-GC. Comparative studies of different redox systems in aqueous electrolyte[5, 6] have established the outer sphere electron transfer mechanism of $Ru(NH_3)_6^{3+}$, the kinetic of which is insensitive to surface modifications. For outer sphere species like $Ru(NH_3)_6^{3+}$, a thin monolayer of adsorbate (<5 Å) would not be expected to have a large effect on the observed electron transfer rates. This is consistent with the observation in Figure SI b that there are minor changes to the CVs of $Ru(NH_3)_6^{3+}$ on PPC-GC and Mix-GC surfaces (thin layers), but a prominent suppression of peak current on OEG-Ph-GC surface (much thicker and multilayers). $Fe(CN)_6^{3-}$, according to literature,[5, 6] requires specific interaction with the electrode surface for electron transfer, therefore, is sensitive to the adsorbed layers, however, the nature of the interaction is insensitive to surface oxidases. More distinct suppression towards the electrochemistry of $Fe(CN)_6^{3-}$ of all 3 modified surfaces, observed in Figure 1a compared to $Ru(NH_3)_6^{3+}$ in Figure 1b, is consistent with the inner sphere electron transfer behavior of $Fe(CN)_6^{3-}$. By comparing PPC-GC, Mix-

GC and OEG-Ph-GC in Figure SI 7 a, the difference of the extent of the suppression to the peak current has indicated different accessibility of the modified layers to $Fe(CN)_6^{3-}$. Mix-GC surface has shown to be significantly more accessible to $Fe(CN)_6^{3-}$ than the other two modified surfaces, indicated a loosely packed thin layers. A noticeable higher suppression of the Mix-GC surface to the anodic peak current of $Fe(CN)_6^{3-}$ than cathodic peak current is observed. The phenomenon cannot be explained at this time but could be due to the slightly increase of the molecular size after $Fe(CN)_6^{3-}$ been reduced to $Fe(CN)_6^{4-}$, to which the grafted layer is slightly less penetrable. A similar observation is also made from the CVs of TMAP-GC in $Ru(NH_3)_6^{3+}$ solution. (Figure SI.2 in supporting information from Gui *et al*.[7])

Impedance Measurement of PPC-GC, Mix-GC, OEG-Ph-GC, OEG-SAM and C12-SAM Surfaces in Aqueous Solution Containing Charged Redox Probes

Although the redox peaks separation in CV can be used to roughly compare the influence of functional layers as a barrier to electron transfer rate of the redox probes, more accurate measurement has been carried out by Faradaic electrochemical impedance spectroscopy (EIS). The measurements were performed in the same $Fe(CN)_6^{3-}$ and $Ru(NH_3)_6^{3+}$ solutions as used in CV measurements. The EIS spectra were run over a frequency range of 0.1-100000 Hz at OCP for $Fe(CN)_6^{3-}$ and an applied DC potential at -0.165 V for $Ru(NH_3)_6^{3+}$, with an amplitude of 10mV.

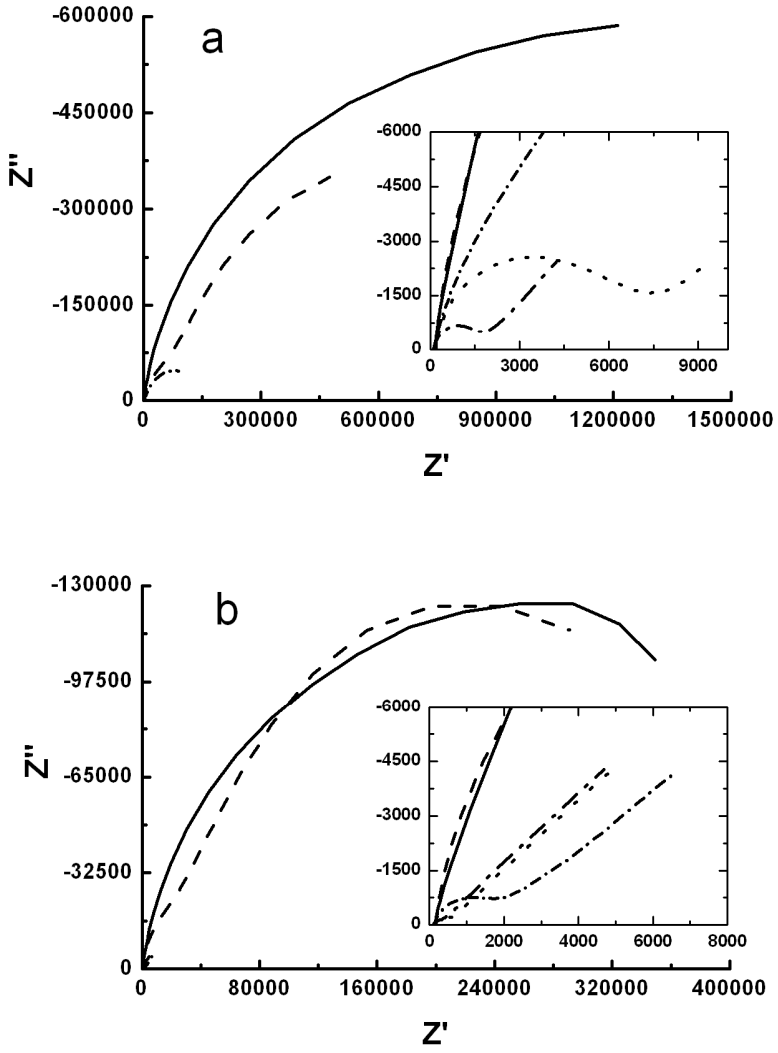

Figure SI 8. EIS Nyquist plots of comparing the Faradaic impedance on PPC-GC (dot curve), Mix-GC (dash dot curve), OEG-Ph-GC (short dash dot curve), OEG-SAM-Au (dash curve) and C12-SAM-Au in (solid curve) (a) 1 mM $Fe(CN)_6^{3-}$ with 0.1 M KCl aqueous solution (b) 1 mM $Ru(NH_3)_6^{3+}$ with 0.1 M KCl aqueous solution.

Figure SI. 8 presents the comparison of EIS result of different surfaces using Nyquist plots. The charge transfer resistance R_{ct}, determined by the size of the semicircle in the plots, can be compared. It is easily identified from the striking differences of the size of the semicircle that the R_{ct} of alkanethiol SAMs on gold to both $Fe(CN)_6^{3-}$ and $Ru(NH_3)_6^{3+}$ are much higher than phenyl layers.

Additional Fluorescence Microscope Images of Protein Adsorption on Electrode Surfaces and Bar Charts of Protein Adsorption Level of Comparison between Individual Samples of Same Surface Chemistry

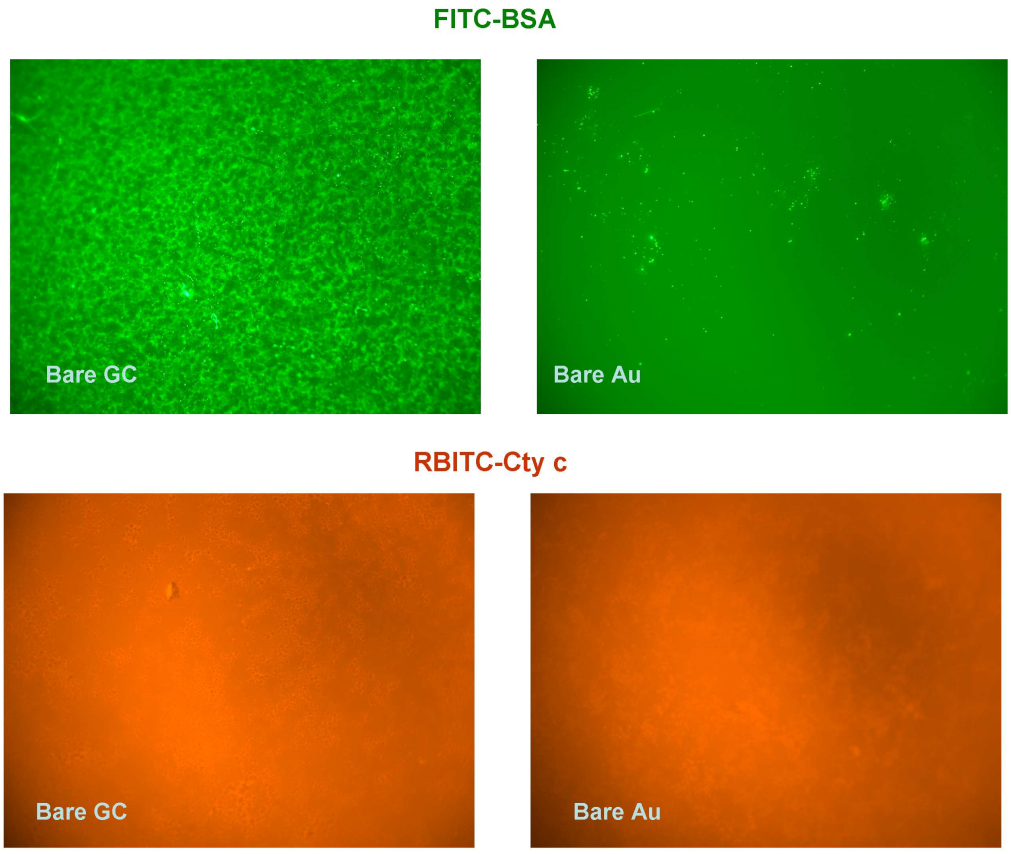

Figure SI 9. Fluorescence microscopic images of FITC-BSA and RBITC-Cyt c adsorbed bare GC and Au surfaces under 63x magnification in the area between bare part (unmodified) and the modified part of the glassy carbon surface.

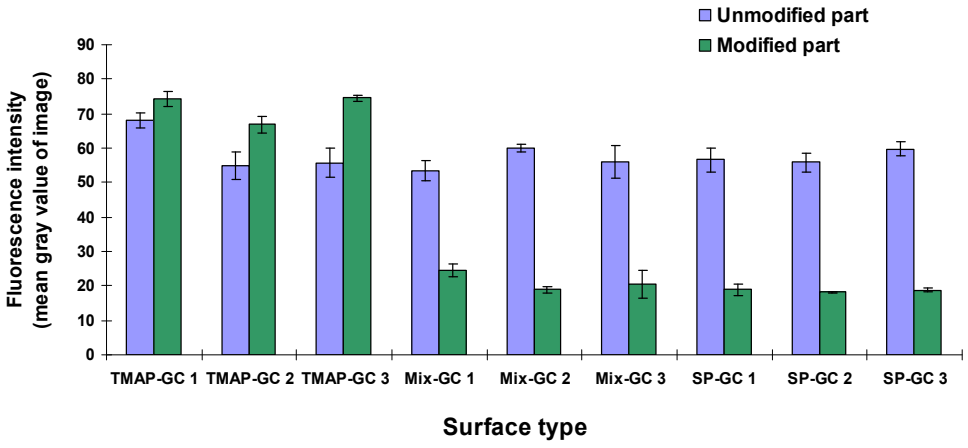

Figure SI 10. Comparison between individual samples in fluorescence intensity of FITC-BSA adsorption on TMAP-GC, Mix-GC and SP-GC surfaces

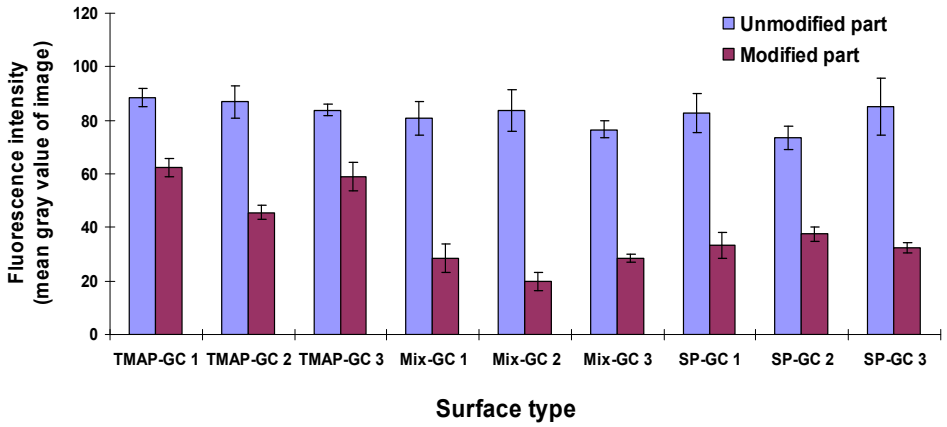

Figure SI 11. Comparison between individual samples in fluorescence intensity of RBITC-Cyt c adsorption on TMAP-GC, Mix-GC and SP-GC surfaces

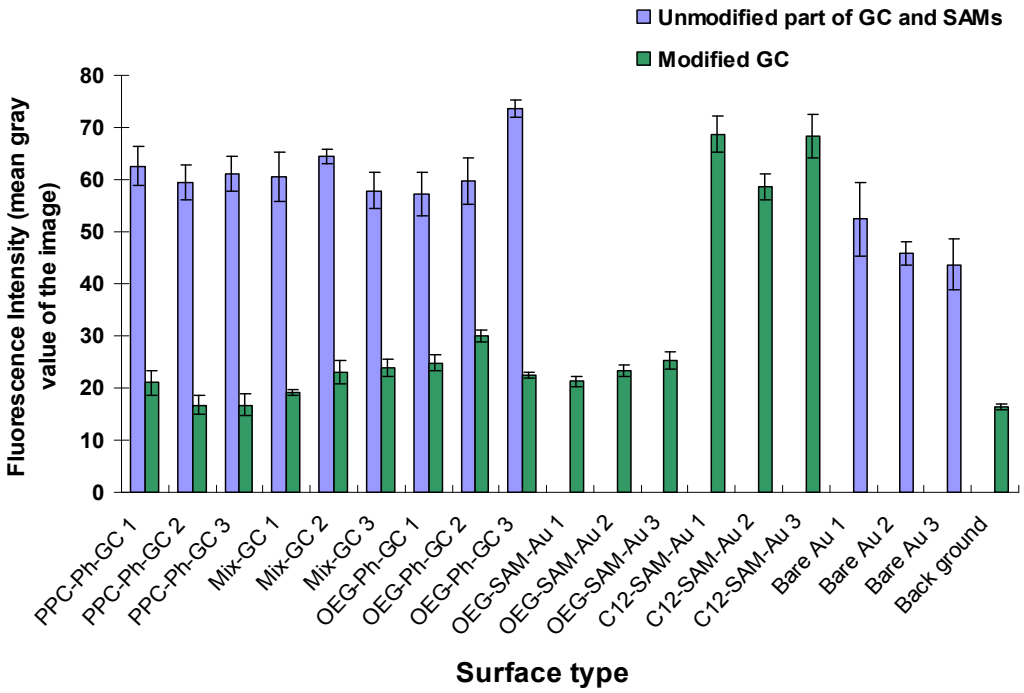

Figure SI 12. Comparison between individual samples in fluorescence intensity of FITC-BSA adsorption on PPC-GC, Mix-GC, OEG-Ph-GC, OEG-SAM-Au, and C12-SAM-Au surfaces

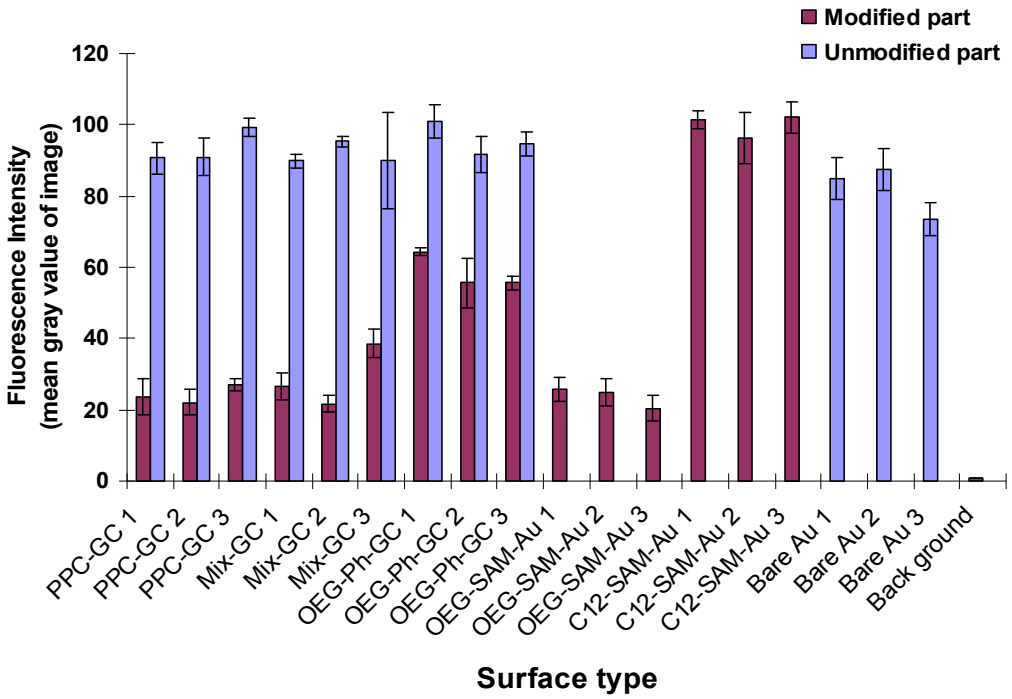

Figure SI 13. Comparison between individual samples in fluorescence intensity of RBITC-Cyt c adsorption on PPC-GC, Mix-GC, OEG-Ph-GC, OEG-SAM-Au, and C12-SAM-Au surface

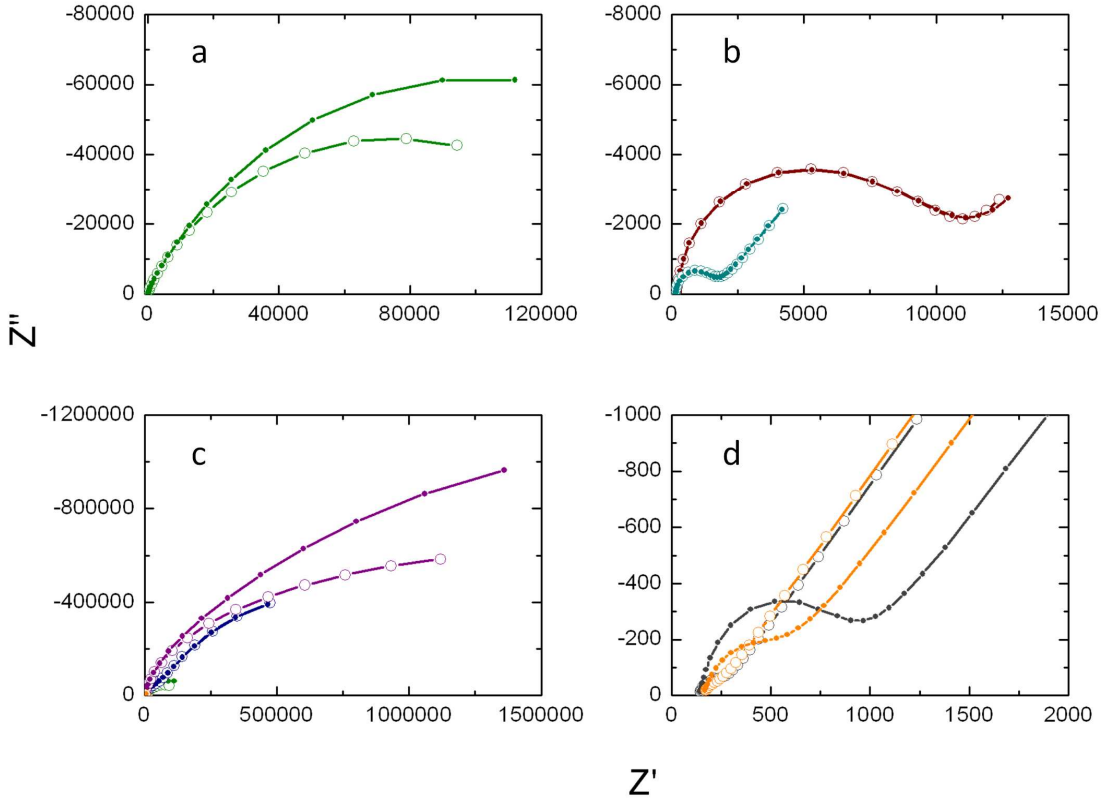

Figure SI 14. EIS Nyquist plots comparing the Faradaic impedance at surfaces of OEG-Ph-GC (a); PPC-GC and Mix-GC (b); OEG-SAM-Au and C12-SAM-Au (c); Bare GC and Bare Au, in 1 mM $Fe(CN)_6^{3-}$ with 0.1 M KCl aqueous solution before (-○-) and after (-●-) adsorption of BSA .

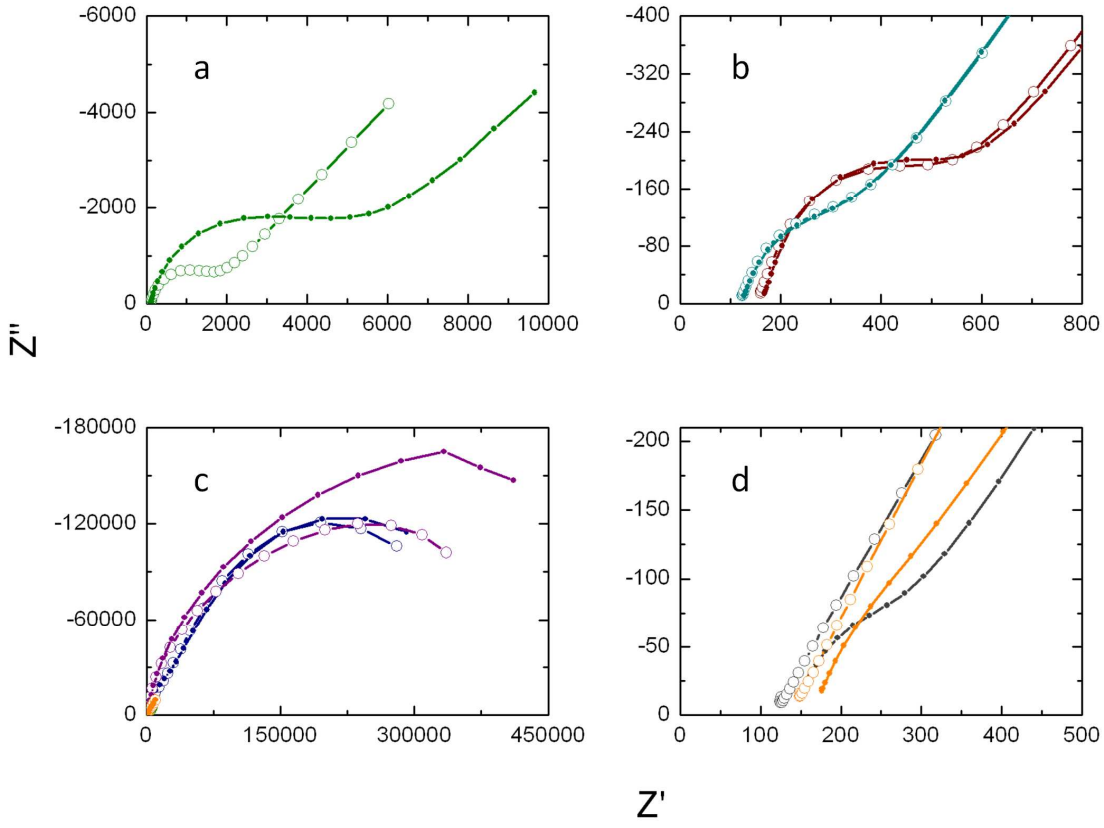

Figure SI 15. EIS Nyquist plots of comparing the Faradaic impedance at surfaces of OEG-Ph-GC (a); PPC-GC and Mix-GC (b); OEG-SAM-Au and C12-SAM-Au (c); Bare GC ad Bare Au, in 1 mM $Ru(NH_3)_6^{3+}$ with 0.1 M KCl aqueous solution before (-○-) and after (-●-) adsorption of BSA.

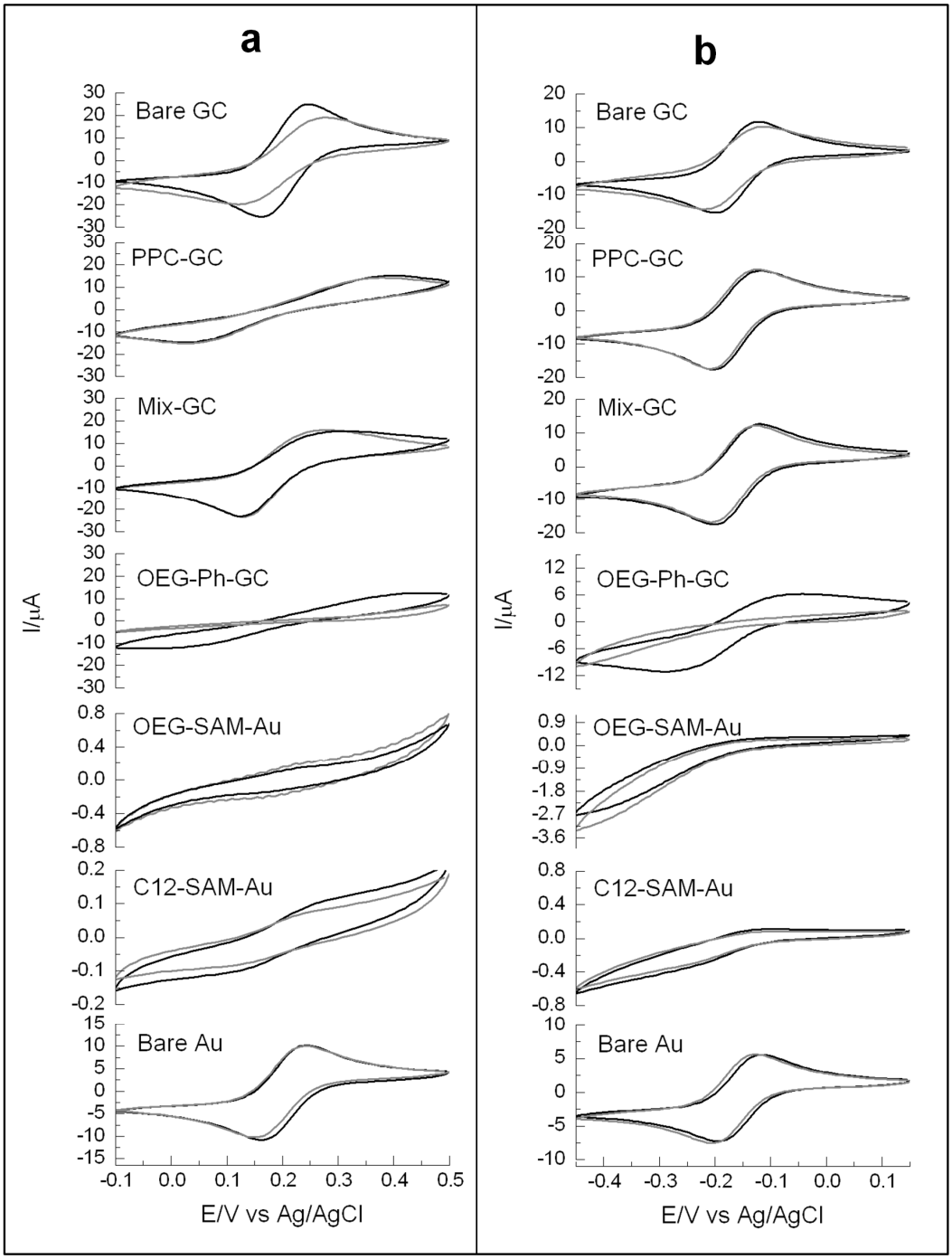

Figure SI 16. Cyclic voltammetry of glassy carbon electrodes in 1 mM $Fe(CN)_6^{3-}$ with 0.1 M KCl aqueous solution (a); 1 mM $Ru(NH_3)_6^{3+}$ with 0.1 M KCl aqueous solution (b), a comparison of various surfaces before (black curve) and after (gray curve) BSA adsorption.

(1) Baranton, S.; Belanger, D. *J. Phys. Chem. B* **2005,** *109,* 24401-24410.
(2) Shewchuk, D. M.; McDermott, M. T. *Langmuir* **2009,** *25,* 4556-4563.
(3) Yu, S. S. C.; Tan, E. S. Q.; Jane, R. T.; Downard, A. J. *Langmuir* **2007,** *23,* 11074-11082.

(4) Shein, J. B.; Lai, L. M. H.; Eggers, P. K.; Paddon-Row, M. N.; Gooding, J. J. *Langmuir* **2009,** *25,* 11121-11128.
(5) Chen, P. H.; McCreery, R. L. *Anal. Chem.* **1996,** *68,* 3958-3965.
(6) Cline, K. K.; Mcdermott, M. T.; Mccreery, R. L. *J. Phys. Chem.* **1994,** *98,* 5314-5319.
(7) Gui, A. L.; Yau, H. M.; Thomas, D. S.; Chockalingam, M.; Harper, J. B.; Gooding, J. J. *Langmuir : the ACS journal of surfaces and colloids* **2013,** *29,* 4772-81.